Electronic Supplementary Material (ESI) for New Journal of Chemistry.
This journal is © The Royal Society of Chemistry and the Centre National de la Recherche Scientifique 2018

Supplementary Information

A new fluorescent-colorimetric chemosensor for cobalt(II) ion based on bis-benzimidazolium salt with three anthraquinone groups

Qing-Xiang Liu,[a,b,*] Ze-Liang Hu[a,b], Zhi-Xiang Zhao[a,b]

[a]*Key Laboratory of Inorganic-Organic Hybrid Functional Materials Chemistry (Tianjin Normal University), Ministry of Education, College of Chemistry, Tianjin Normal University, Tianjin 300387, China*

[b]*Tianjin Key Laboratory of Structure and Performance for Functional Molecules, College of Chemistry, Tianjin Normal University, Tianjin 300387, China.*

*Corresponding Author.

E-mail address: tjnulqx@163.com (Q. Liu).

Table of contents

1. CCDC number for **3**.
2. Summary of crystallographic data for **3** (Table S1).
3. The UV/Vis and fluorescence studies of **3** (Fig. S1-Fig. S7).
4. HRMS spectra for **3**·Co^{2+} (Fig. S8).
5. The infrared spectra of **3** and **3**·Co^{2+} (Fig. S9).
6. The ^{1}H NMR and ^{13}C NMR spectra of intermediates and compound **3** (Fig. S10-Fig. S16).

1. CCDC number for 3.

CCDC 1854484 contains the supplementary crystallographic data for compound **3** These data can be obtained free of charge via http//www.ccdc.cam.ac.uk/conts/retrieving. html, or from the Cambridge Crystallographic Data Centre, 12 Union Road, Cambridge, CB2 1EZ, UK; fax: (+44) 1223-336-033; or e-mail: deposit@ccdc.cam.ac.uk.

2. Summary of crystallographic data for 3.

Table S1 Summary of crystallographic data for **3**

Chemical formula	$C_{64}H_{46}F_{12}N_4O_{12}P_2$	F(000)	2768.0
Fw	1352.99	Cryst size, mm	0.25 × 0.22 × 0.2
Cryst syst	Monoclinic	θ_{min}, θ_{max}, deg	4.164, 50.02
Space group	$P2_1/c$	T /K	150.0(1)
a/Å	23.954 (1)	No. of data collected	25490
b/Å	12.411 (6)	No. of unique data	9847
c/Å	19.019 (9)	No. of refined params	849
α/deg	90	Goodness-of-fit on F^2	0.957
β/deg	98.305(4)	Final R indices[b] [$I > 2\sigma(I)$]	
γ/deg	90	$R1$	0.0418
V/Å^3	5595.4(5)	$wR2$	0.0867
Z	4	R indices (all data)	
D_{calcd}, Mg/m^3	1.606	$R1$	0.0707
Abs coeff, mm^{-1}	0.191	$wR2$	0.0989

[a]GOF = $[\Sigma\omega(F_o^2 - F_c^2)^2 /(n - p)]^{1/2}$, where n is the number of reflection and p is the number of parameters refined. [b]$R_1 = \Sigma(||F_o| - |F_c||)/\Sigma|F_o|$; $wR_2 = [\Sigma[w(F_o^2 - F_c^2)^2]/ \Sigma w(F_o^2)^2]^{1/2}$.

3. The UV/Vis and fluorescence studies of compound 3.

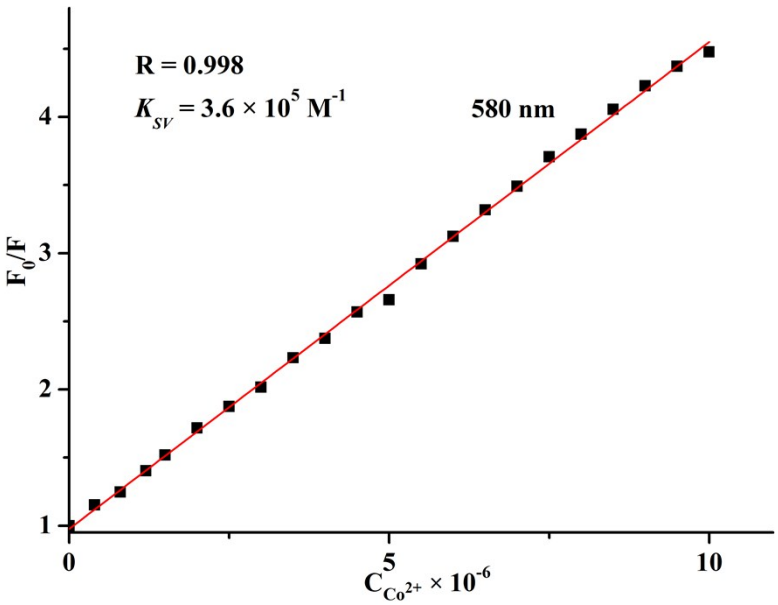

Fig. S1 Stern-Volmer plot describing **3** increasing caused by Co^{2+} association in CH_3CN solutions at 580 nm. The K_{SV} is 3.6×10^5 M^{-1}, and the linear range is from 0-10.0×10^{-6} mol/L.

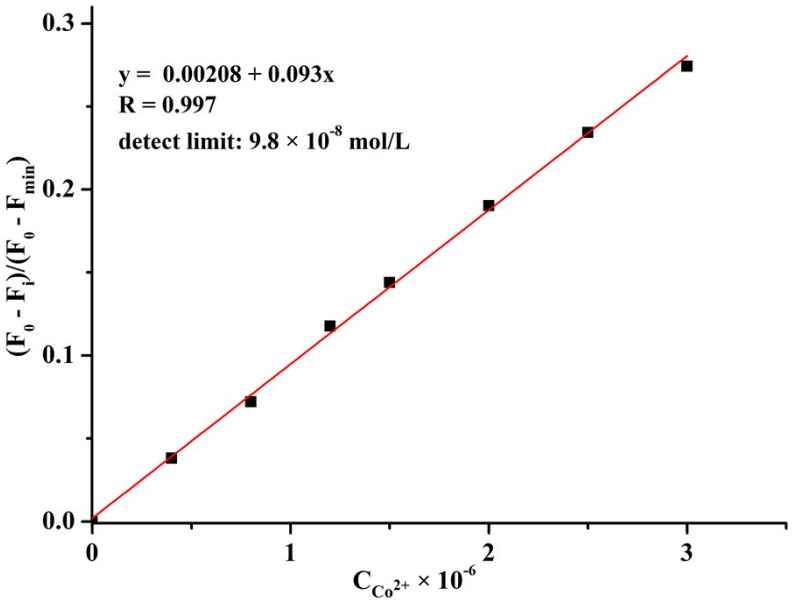

Fig. S2 Emission (at 410 nm) of **3** at different concentrations of Co^{2+} (0.0, 0.4, 0.8, 1.2, 1.5, 2.0, 2.5, 3.0 × 10^{-6} M) added, normalized between the minimum emission (0.0 M Co^{2+}) and the emission at 3.0 × 10^{-6} M Co^{2+}. The detection limit was determined to be 0.098 μM.

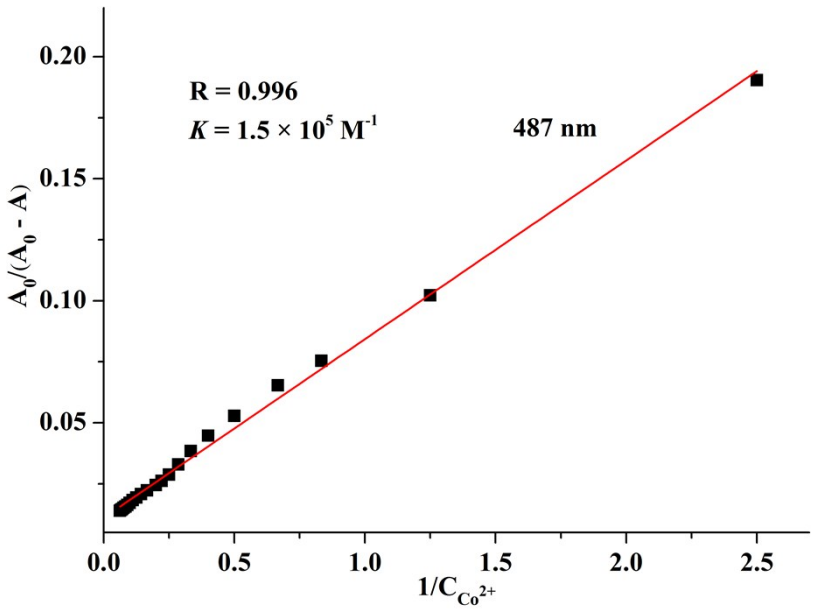

Fig. S3 Benesi-Hildebrand plots assuming 1:1 stoichiometry between **3** and Co^{2+}.

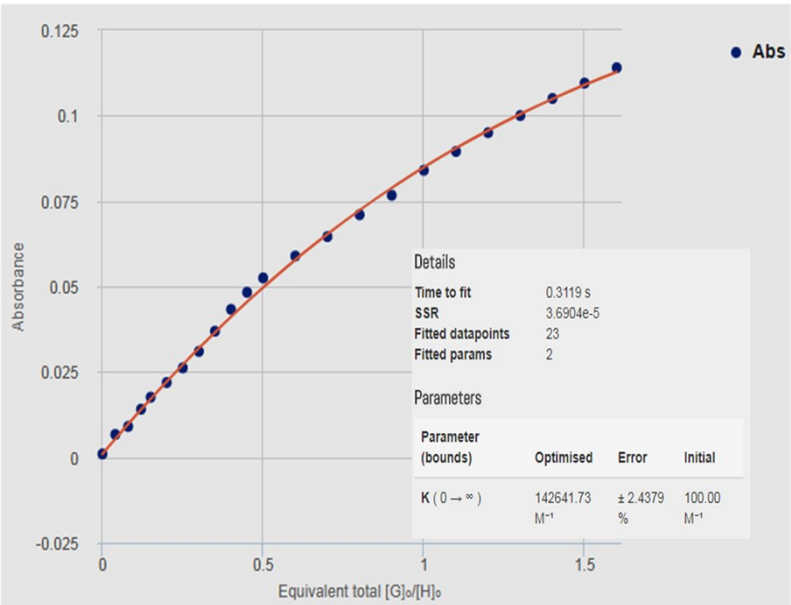

Fig. S4 Binding constant of the **3**·Co^{2+} was calculated from the online (BindFit v0.5) server based on UV 1:1 model.

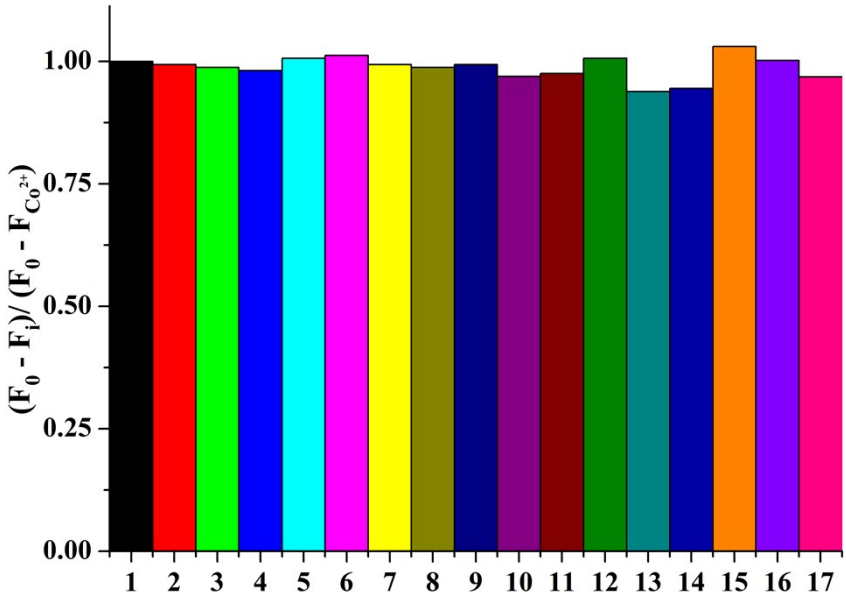

Fig. S5 Change ratio $(F_0 - F_i)/(F_0 - F_{Co^{2+}})$ of fluorescence intensity at 580 nm of **3** upon addition of 2.0 equiv. Co^{2+} in the presence of 2.0 equiv. of background cations. 1: Co^{2+}; 2: Co^{2+} + Li^{+}; 3: Co^{2+} + Na^{+}; 4: Co^{2+} + K^{+}; 5: Co^{2+} + NH_4^{+}; 6: Co^{2+} + Ag^{+}; 7: Co^{2+} + Ca^{2+}; 8: Cu^{2+} + Ni^{2+}; 9: Co^{2+} + Cu^{2+}; 10: Co^{2+} + Zn^{2+}; 11: Co^{2+} + Cr^{3+}; 12: Co^{2+} + Cd^{2+}; 13: Co^{2+} + Al^{3+}; 14: Co^{2+} + Pb^{2+}; 15: Co^{2+} + Hg^{2+} ; 16: Co^{2+} + Fe^{2+}; 17: Co^{2+} + Fe^{3+} in CH_3CN at 25 ˚C.

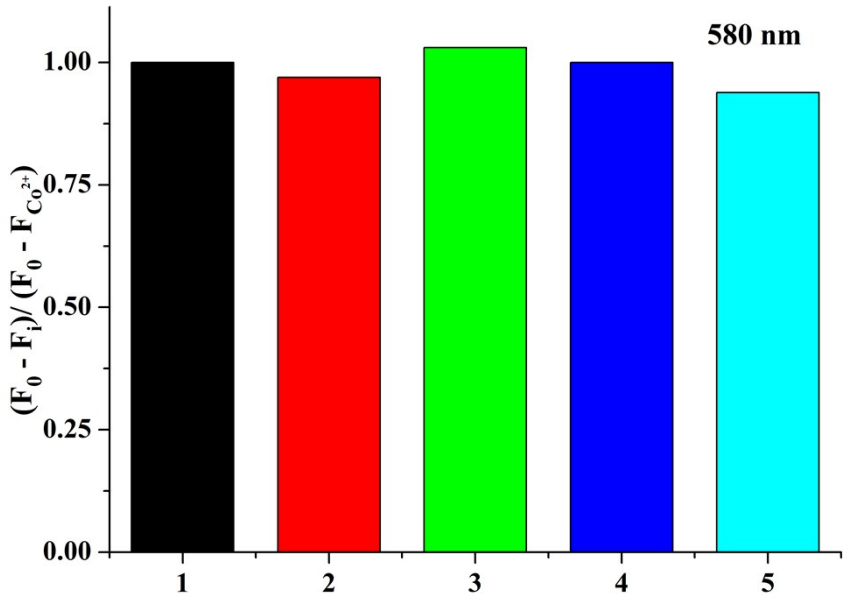

Fig. S6 Fluorescence intensity of **3** (5.0×10^{-6} mol/L) in various mixtures of different Co^{2+} salts (10.0×10^{-6} mol/L) in CH_3CN at 25 ˚C. (1): $Co(NO_3)_2$; (2): $CoSO_4$; (3): $CoBr_2$; (4): $Co(OAc)_2$; (5): $CoCl_2$.

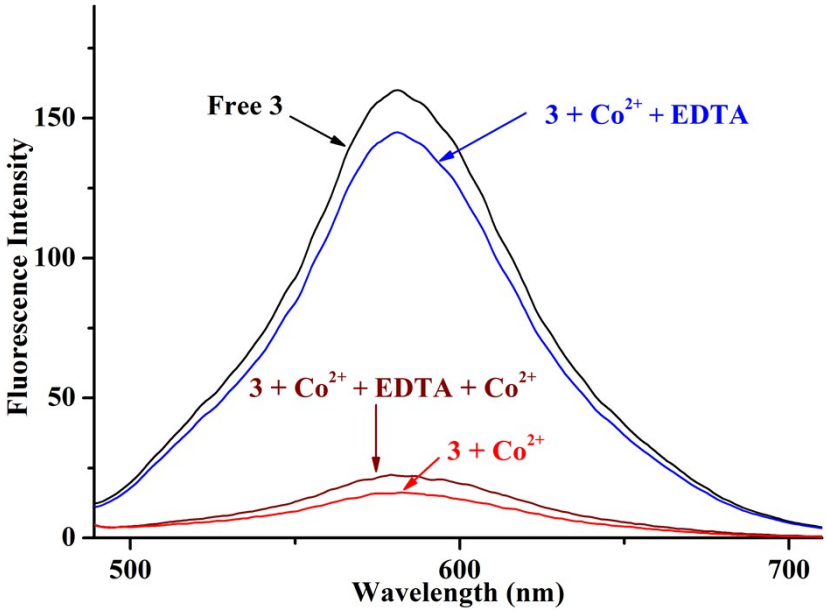

Fig. S7 Fluorescence reversibility of **3** upon the detection of Co^{2+}. Fluorescent changes of **3** after the addition of Co^{2+}, EDTA, Co^{2+} in that order in CH_3CN at 25 ˚C.

4. HRMS spectra for 3·Co^{2+}.

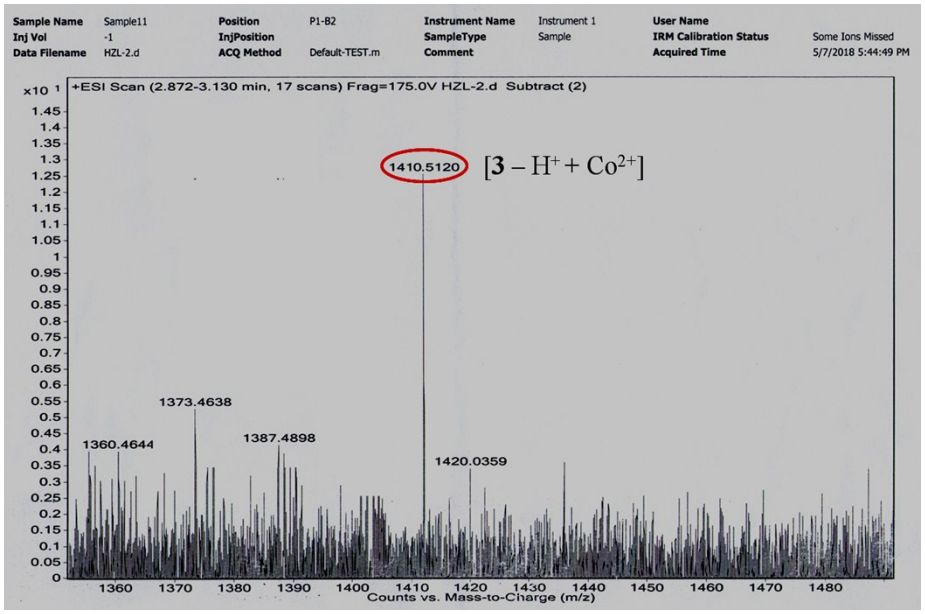

Fig. S8 HRMS spectra for **3**·Co^{2+}. MS (EI): [**3** – H^+ + Co^{2+}] = 1410.5120.

5. The infrared spectra of 3 and 3·Co^{2+}.

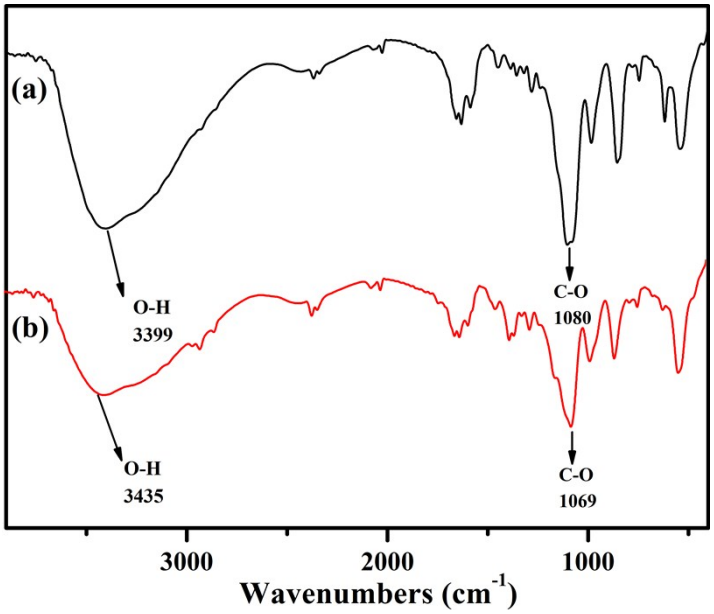

Fig. S9. Infrared spectra of (a) **3**; (b) **3**·Co^{2+}.

6. The ^{1}H NMR and ^{13}C NMR spectra of intermediates and compound 3.

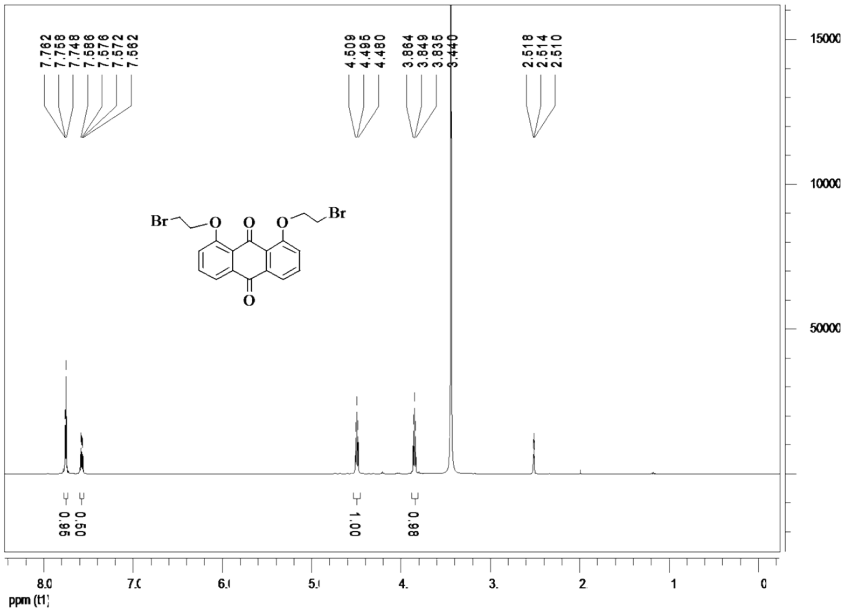

Fig. S10 The ^{1}H NMR (400 MHz, DMSO-d_6) spectra of 1,8-di(2-bromoethoxy)-9,10-anthraquinone.

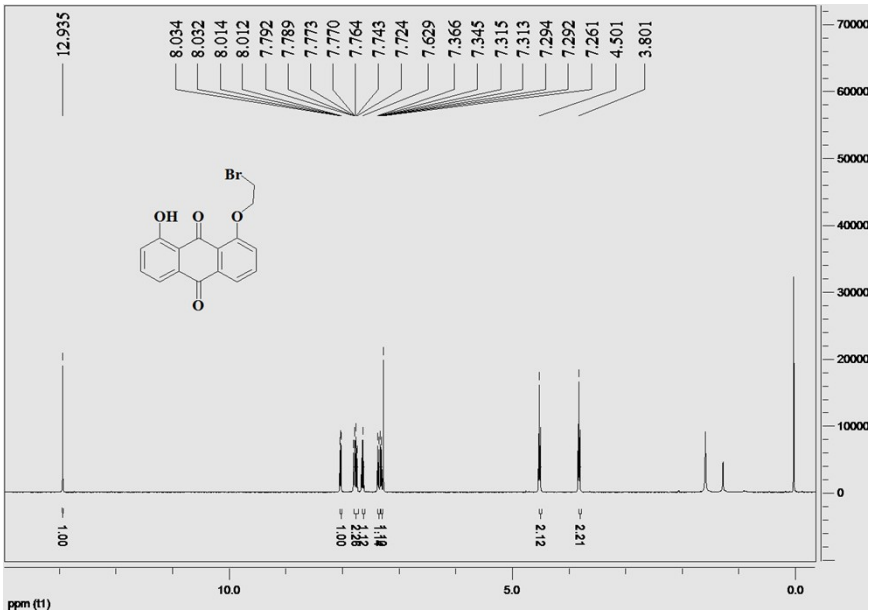

Fig. S11 The ^{1}H NMR (400 MHz, $CDCl_3$) spectra of 1-(2-bromoethoxy)-8-hydroxy-9,10-anthraquinone (**1**).

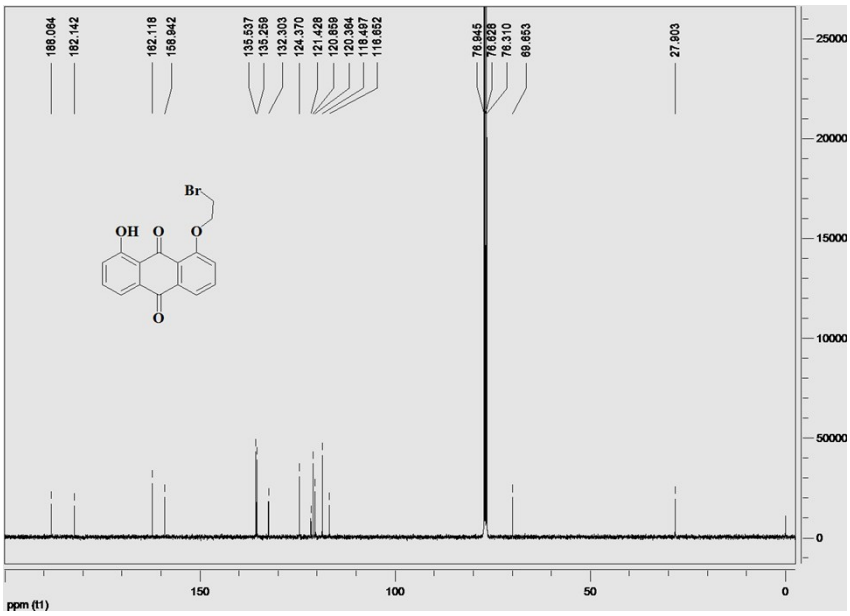

Fig. S12 The ^{13}C NMR (100 MHz, $CDCl_3$) spectra of 1-(2-bromoethoxy)-8-hydroxy-9,10-anthraquinone (**1**).

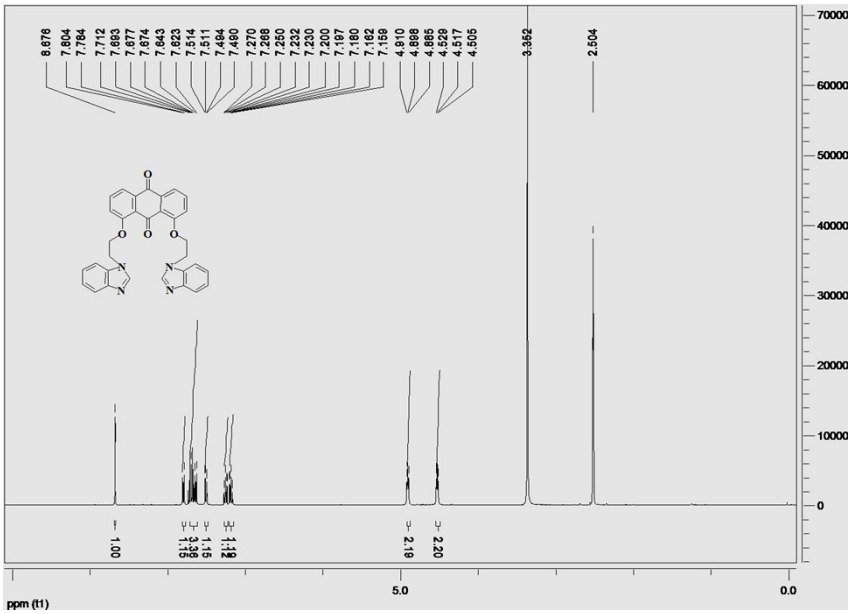

Fig. S13 The ^{1}H NMR (400 MHz, DMSO-d_6) spectra of 1,8-bis[2-(benzimidazol-1-yl)ethoxy]-9,10-anthraquinone (**2**).

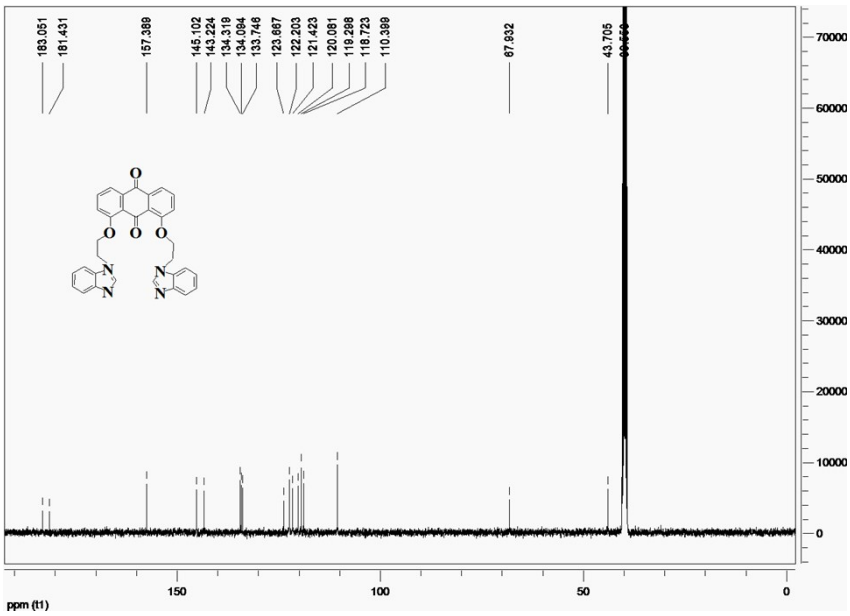

Fig. S14 The ^{13}C NMR (100 MHz, DMSO-d_6) spectra of 1,8-bis[2-(benzimidazol-1-yl)ethoxy]-9,10-anthraquinone (**2**).

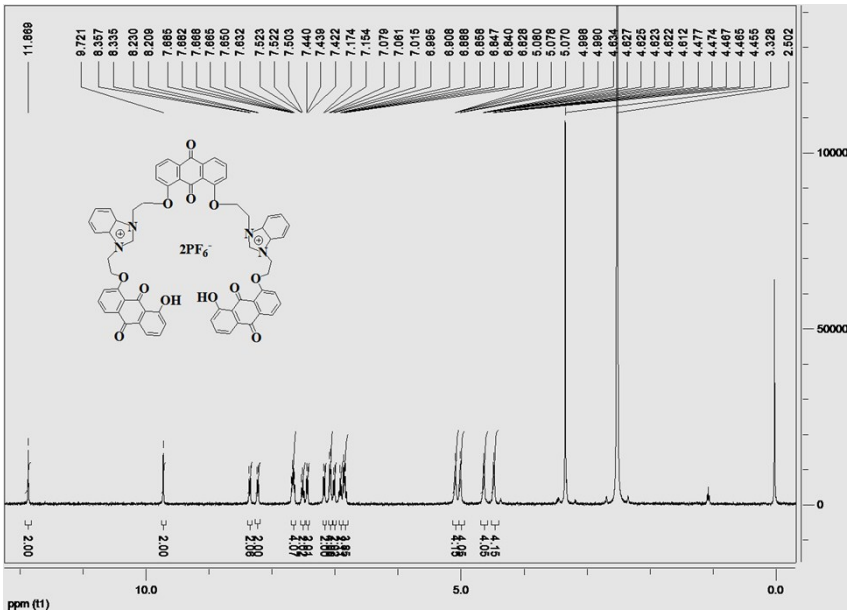

Fig. S15 The ^{1}H NMR (400 MHz, DMSO-d_6) spectra of compound **3.**

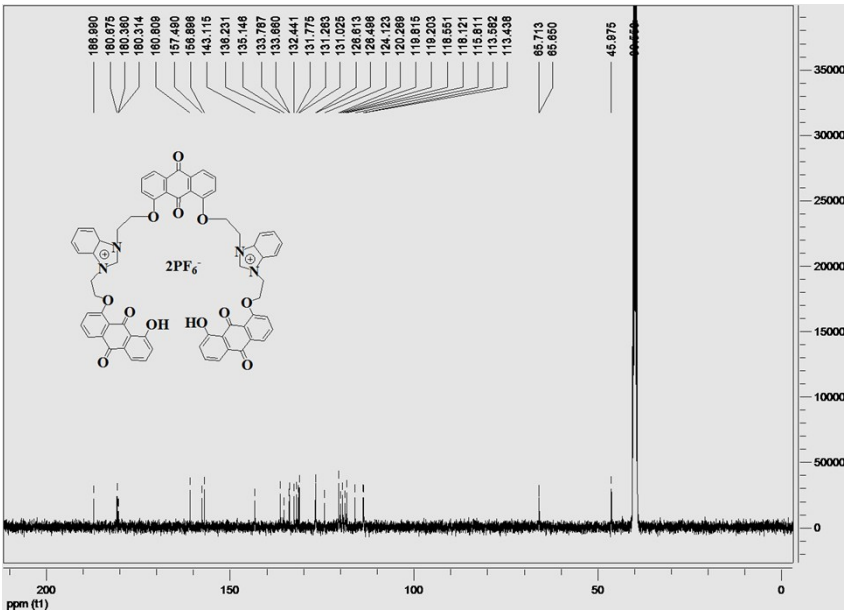

Fig. S16 The ^{13}C NMR (100 MHz, DMSO-d_6) spectra of compound **3.**